HYDROLOGICAL PROCESSES
Hydrol. Process. **19**, 1007–1019 (2005)
Published online in Wiley InterScience (www.interscience.wiley.com). DOI: 10.1002/hyp.5642

Rainfall monitoring systems over an urban area: the city of Rome

Fabio Russo,[1]* Francesco Napolitano[1] and Eugenio Gorgucci[2]

[1] *Department of Hydraulics, Transportations and Roads, University of Rome 'La Sapienza', 00184 Rome, Italy*
[2] *Institute of Atmospheric Sciences and Climate, National Research Council, 00133 Rome, Italy*

Abstract:

In small catchments a very high space–time rainfall resolution is needed in order to obtain, with sufficient accuracy, flash flood nowcasting as well as monitoring of sewer systems. In this light, a radar meteorology campaign was conducted during the fall of 2001, over the city of Rome (Italy), using measurements collected by the polarimetric Doppler radar Polar 55C located in the south-east of the city at a distance of 15 km from the downtown and by a network consisting of 32 tipping bucket raingauges. A comparative analysis of the rainfall fields obtained using two interpolation methods (inverse-distance and kriging) with those obtained using radar rainfall measurements was performed. The overall performance of the different methods was evaluated using objective functions. Errors depending on the gauge density were weighed by changing the number of raingauges considered in the reconstructed rainfall fields. Copyright © 2005 John Wiley & Sons, Ltd.

KEY WORDS rainfall fields; weather radar; raingauge network; rainfall interpolation

INTRODUCTION

Rainfall estimation over a catchment area from data taken at several measurement stations is an important stage in many hydrological applications (Bras and Rodriguez-Iturbe, 1976; Chua and Bras, 1982; Bastin *et al*., 1984). In fact one of the most important limits of hydrological prediction is determined by the input of hydrological models (Paoletti, 1993; Vaes *et al*., 2001). This input is given by raingauge measurements so that the accuracy of the output depends essentially on the raingauge network density, configuration and on the instrument accuracy (Maheepala *et al*., 2001). To estimate the rainfall fields over an entire basin, raingauge pointwise measurements need to be interpolated and different interpolation methods can lead to significant differences in rainfall estimation (Dirks *et al*., 1998).

The small-scale variability of rainfall fields leads to biases on the rain rate estimation over an entire basin, above all for small or medium-size mountainous and urban catchments (Borga *et al*., 2000; Todini, 1995). In this context, weather radars have several advantages since a single site is able to obtain coverage over a vast area with very high temporal and spatial resolution and the advent of weather radar systems with better beam resolution, increased signal-to-noise sensitivity, faster volume scan cycles and dual polarization capability allowed progress on radar rainfall estimation (Anagnostou and Krajewski, 1999) and its hydro-meteorological applications (Finnerty *et al*., 1997).

In this light the problems of optimization of raingauge networks and interpolation techniques could be considered rather out-of-date, as nowadays weather radar provides an estimation of rainfall rates with excellent spatial and temporal resolution (Pardo-Igùzquiza, 1998). However, a complete coverage by radar is still limited to some western countries and anyway radar rainfall estimates over mountainous regions are still a difficult

* Correspondence to: Fabio Russo, Dept. of Hydraulic, Transportations and Roads, University of Rome "La Sapienza", Via Eudossiana 18, 00184 Rome, Italy. E-mail: fabio.russo@uniroma1.it

Received 1 December 2002
Accepted 1 January 2004

task due to the requirements of avoiding beam blockage as well as contamination by the melting layer (Gorgucci *et al*., 1996). Furthermore, it is well known that radar and raingauges go through fundamentally different processes to estimate rain. Raingauges collect water over a period of time, whereas radar obtains instantaneous snapshots of electromagnetic backscatter from rain volumes that are then converted to rainfall via some algorithms.

Spatial and temporal averaging of radar and raingauge data has always been used to reduce the measurement errors and the discrepancy between radar and raingauge estimates. Therefore, extensive analysis of space–time averaging of rainfall over the basin is conducted to study the error structure of the comparison between radar and gauges.

The sampling differences between radar and raingauges give significant uncertainty in rainfall amount estimations, above all in short time intervals; in fact the correlation distance of the rainfall process increases when the rainfall is integrated over longer periods (Krajewski, 1995; Steiner *et al*., 1999). For the same reasons it is also important to observe that raingauge adjustment is really effective for stratiform events and in particular when orographic precipitations are not relevant (Fox *et al*., 1999). Rainfall intermittence and its scaling properties, depending above all on climatology and meteorological conditions, affect the transformation of point to areally averaged rainfall (Krajewski, 1995). From a hydrological point of view it is relevant to say that if rainfall–runoff models, commonly calibrated using historical gauge data, give satisfactory performances, it is acceptable that on average radar estimations should not deviate too far from raingauge measurements. For these reasons both radar and raingauges are important in hydrological applications: radar needs calibration that can be provided using raingauges while the gauges are usually too sparse to detect high rainfall variability.

The paper is organized as follows. The next section presents the rainfall monitoring system over Rome based on the polarimetric Doppler radar Polar 55C located in the south-east of the city at a distance of 15 km from the downtown and on a raingauge network with 32 tipping bucket gauges. Then the principal characteristics of the case study event are briefly described. Subsequently, the following section presents the pointwise comparison between radar and raingauges as well as the comparative analysis of the rainfall fields obtained with the raingauges, using inverse-distance and kriging methods and the corresponding fields obtained using the radar. In the last section we summarize the key results of this paper.

RAINFALL MONITORING OVER THE METROPOLITAN AREA OF ROME

Description of the site

The metropolitan area of Rome presents peculiar climatic characteristics due to the presence of the 'Tirreno' sea to the east, the 'Appennino' mountains to the east, and the 'Colli Albani' hills to the south. Furthermore, the area presents a complex orography itself so that rainfall fields are highly variable. This variability can be observed using the raingauge network, operating over this area with a high spatial and temporal resolution, and with the weather radar.

The raingauge network

In order to improve the predictability of rainfall and floods and to manage the real time control (RTC) of the urban drainage systems, different raingauge networks were merged to obtain a network with 32 tipping buckets. The rainfall accumulation for each raingauge is provided in real time with a resolution of 0·2 mm. The raingauges are distributed throughout the area, with a distance ranging between 5 km and 35 km from the radar.

The weather radar

The existing monitoring network is integrated with the weather radar managed by the Institute of Atmospheric Sciences and Climate of the National Research Council. The Polar 55C is a C-band (5·5 GHz,

$\lambda = 5{\cdot}4$ cm) Doppler dual polarized coherent weather radar with polarization agility and with a $0{\cdot}9^\circ$ beamwidth. Figure 1 shows the position of the radar that is located in the south-east of Rome at a distance of 15 km from the downtown in the 'Tor Vergata' research area (41°50′24″N, 12°38′50″E, 102 m a.s.l.) and the location of the 32 raingauges.

Preliminary analyses on plan position indicators (PPI) collected at different elevations were performed in order to find the best antenna elevation for radar rainfall estimation (Gorgucci *et al*., 1995; Russo *et al*., 2001). In fact, radar scans have to be done at fairly low elevation angles to avoid contamination of radar echoes from the melting layer. At the same time, low-elevation radar scans suffer from ground clutter contamination and blockage of the radar beam from elevated ground targets or mountains. While contamination from ground clutter can be removed using a filter, no processing procedure can recover the blocked echo. When the beam is completely blocked by mountains there will be no radar echo received from the farther targets in the range, and this feature can easily be spotted on radar pictures. However, when the beam is partially blocked the echo received from the ranges farther than the blocking target will be reduced and the radar reflectivity (Z_h) will also be correspondingly reduced proportionally to the amount of the beam blockage. Partially blocked beams may not be easily observed on a radar map because it is difficult to distinguish between a partially blocked echo from a strong target and a weaker weather echo.

The radar operational elevation angle for precipitation estimation is chosen in such a way that on average the beam blocking is minimized and at the same time the radar beam does not suffer from melting layer contamination. The operational mode is obtained by compromising between the above two requirements, and

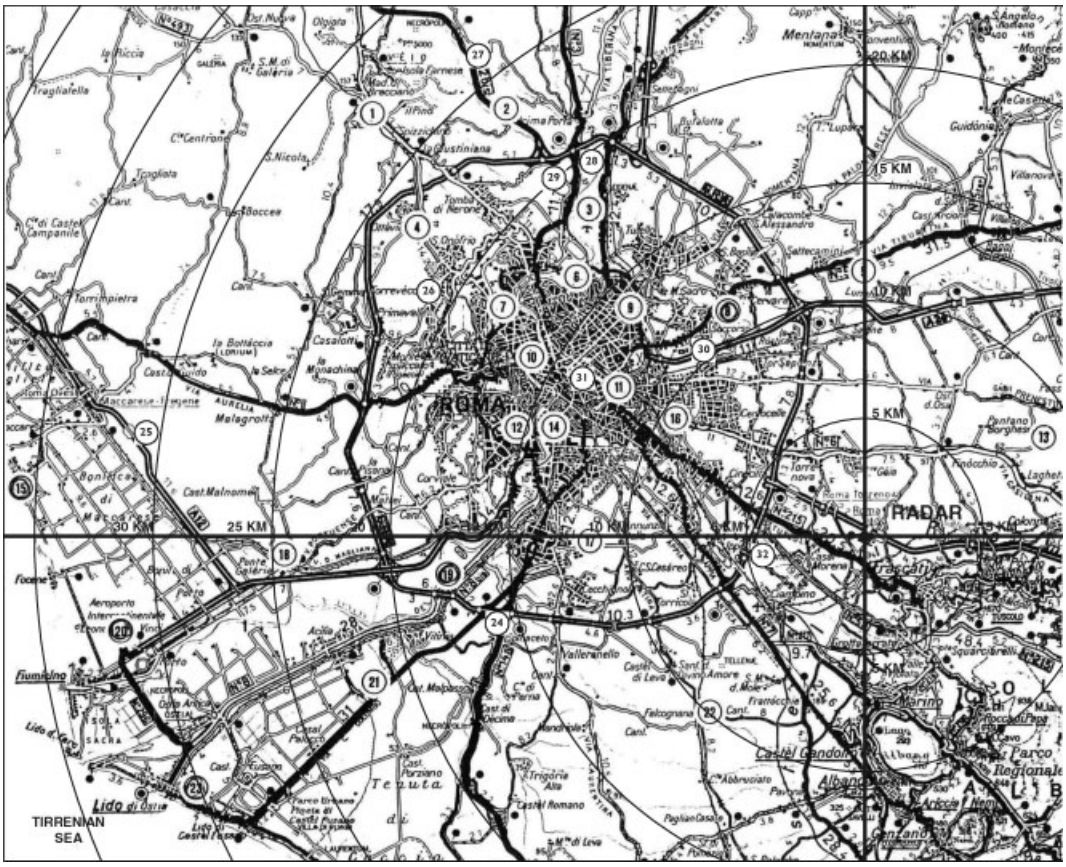

Figure 1. The position of the radar, south-east of Rome, and the location of the 32 raingauges

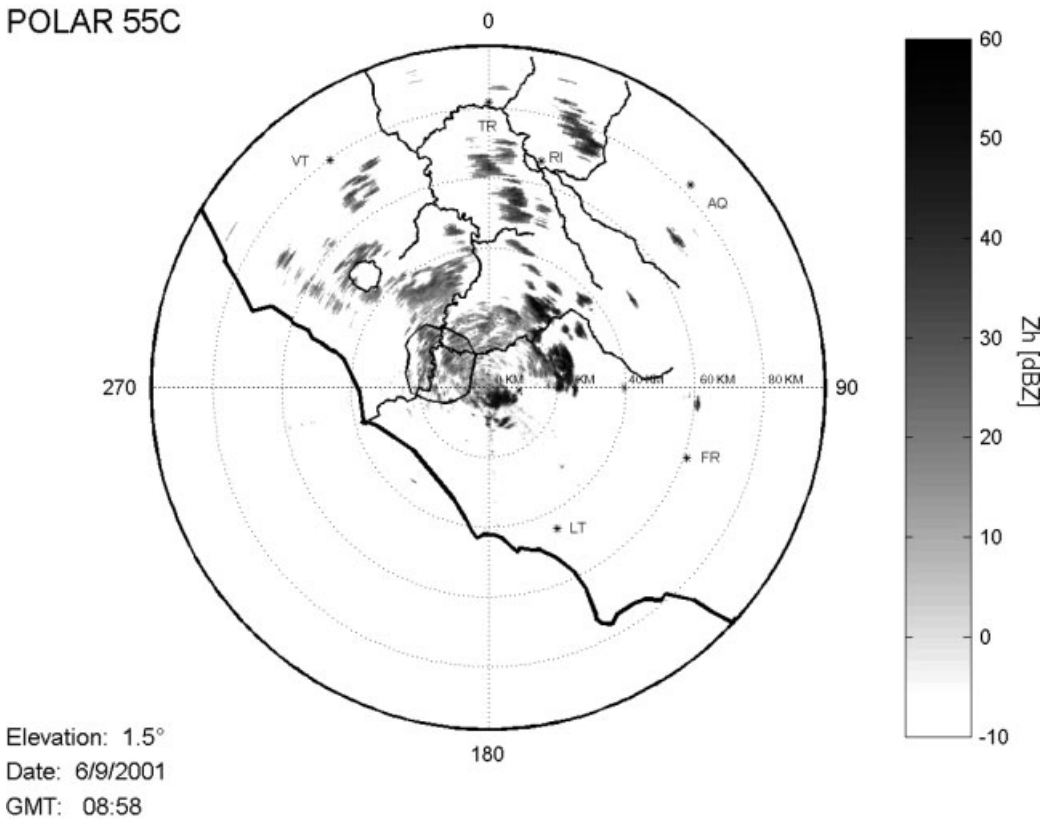

Figure 2. PPI collected on a sunny day in which it is possible to recognize the presence of clutter

the scans are made at an elevation of about 1·8° (some little differences from this value are due to the strong wind). Also, at this elevation some clutter was recognized as shown in Figure 2, where a radar reflectivity map collected on a sunny day is represented: the visibility is reduced in the area to the south-east (azimuth 154°, range 5–15 km) due to the presence of the 'Colli Albani' hills and to the east (azimuth 70–90°, range 20 km) due to the presence of the 'Monti Prenestini' mountains.

CASE STUDY

The data presented in this paper were collected during a precipitation event that occurred on 10 November 2001 over Central Italy, covering a time period of 5 h. The event was associated with the passage of a frontal perturbation that originated in the Atlantic Ocean and moved north-east towards the Mediterranean areas until its arrival in Central Italy. This event was characterized by the presence of very unstable masses of warm moist air. The storm associated with this event produced rainfall over the Tiber basin, creating flood warnings in some areas of the catchment. The precipitation was more intense in the early morning, becoming less and finishing around 2 : 00 p.m.; the rainfall distribution was not uniform over the target area.

During this event, the Polar 55C was put in 'operational mode' to monitor the surrounding areas for hydrological applications. This mode consisted of a scan strategy as follows. PPI scans were done over the full 360° in azimuth at the fixed elevation of 1·8°. The time interval between the PPI scans was set at 5 min to sample the storm system adequately. The radar measurements were obtained by integrating 64 sample pairs

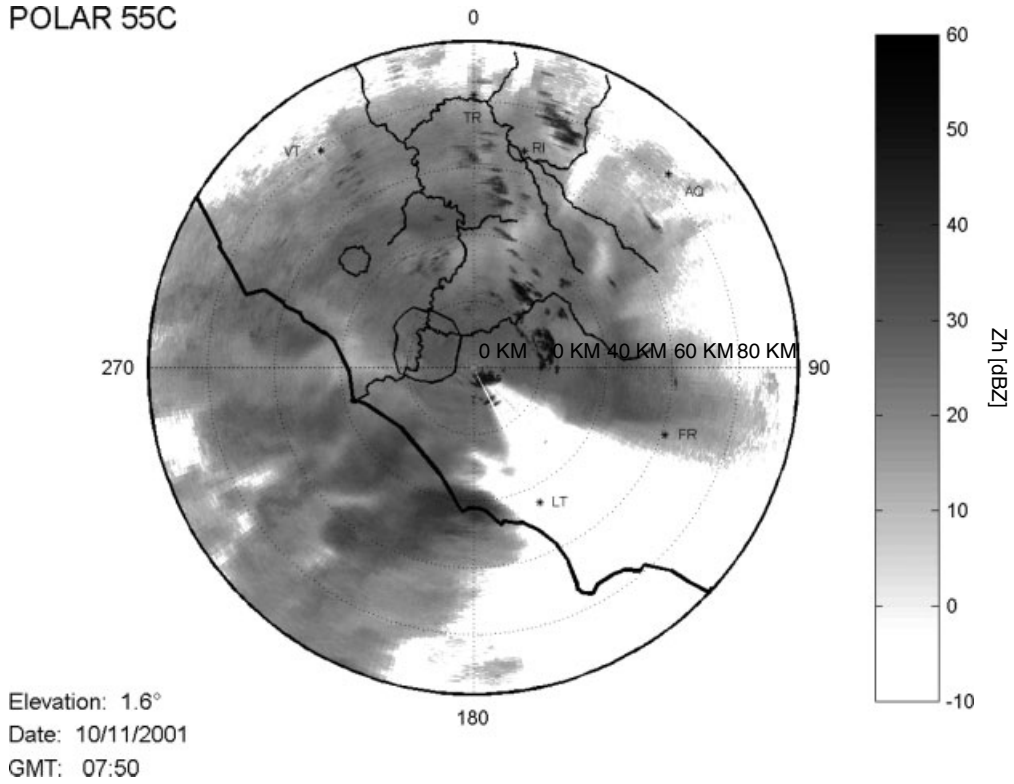

Figure 3. PPI collected on a rainfall day without clutter filtering

of radar returns with a pulse repetition time (PRT) of 0·85 ms. The archived parameters were the reflectivity at horizontal polarization, the differential reflectivity, the mean Doppler velocity and spectral width.

Several preprocessing data reduction procedures were applied to the radar data as described below. The radar reflectivity was thresholded at −10 dBZ to avoid possible noise contamination. This procedure can potentially remove good data close to the radar, where the −10 dBZ levels could be above noise. However, the regions of the storm with these reflectivity levels do not contribute significantly to rainfall and therefore can be ignored for our applications. Second, potential contamination from hail/ice regions was eliminated, enforcing an upper limit of 55 dBZ for the reflectivity factor (Aydin *et al*., 1986). Again here the loss of good data points near the boundary is outweighed by potentially erroneous data that can bias the rainfall estimates significantly. Third, potential ground clutter contamination was removed with an algorithm that was found in order to filter the radar measurements, and is based on the backscattering signal variance of the differential reflectivity: the meteorological targets have a standard deviation of about ±0·2 dBZ while for ground clutter this value increases significantly with the orographic gradient. In the cells affected by ground clutter the measurements were averaged over the nearest neighbours up to 2 km on either side to reduce the measurement error fluctuations. Figures 3 and 4 show a reflectivity map with and without the clutter filter.

DATA ANALYSIS AND EXPERIMENTAL RESULTS

Pointwise comparison between raingauge measurements and radar estimates

Radar PPIs are obtained nearly instantaneously, whereas raingauge data are obtained as an accumulation over finite time intervals. With a scan rate of $6^\circ\ s^{-1}$ it takes 1 min to get a PPI, whereas the raingauge

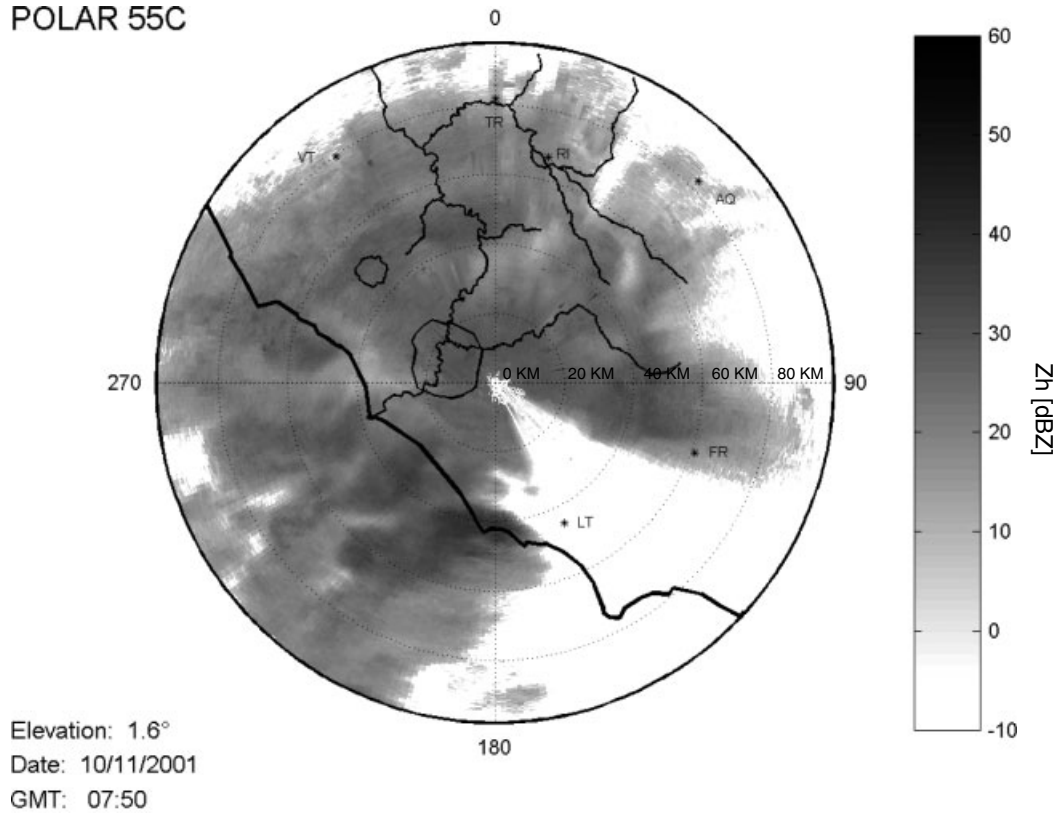

Figure 4. PPI collected on a rainfall day with clutter filtering

data in this data set is integrated over 30 min. Therefore, to enable proper comparison between radar and raingauge data, the following procedure is adopted: a time series of radar data was constructed at the gauge locations from the instantaneous snapshots of the PPIs and then this time series was interpolated to provide the time synchronization between radar and raingauge data. Figure 5 shows a sample time series of accumulated rainfall constructed for a raingauge and the corresponding radar estimates R_{Zh} at the gauge location.

Despite intrinsic problems in the radar and raingauge rainfall comparison, caused by sampling volume differences and the small-scale variability of rainfall, data from raingauges are used to adjust the radar rainfall estimates from reflectivity in the vicinity of a gauge. In this work the adjustment of radar data is obtained by matching mean accumulations of radar rainfall estimations at raingauge sites with the total rainfall measured by the gauge. This procedure can influence the generally good comparison of rainfall fields because the radar fields are forced to be closer to raingauge ones, but in this way it is possible to correlate every difference between the raingauge rainfall fields and the radar generated fields in the cells without raingauges, with better radar capability to describe rainfall spatial variability.

The location of each raingauge is collocated with the corresponding radar PPI reflectivity factor. Subsequently, the radar data are converted to rainfall rates using an appropriate algorithm. The algorithm used in this study is based on a $Z-R$ relation found by simulation. Rainfall values, ranging from 0 to 300 mm h^{-1}, are simulated varying the parameters of the gamma raindrop size distribution (RSD) over a wide range, as suggested by Ulbrich (1983). For each RSD the corresponding Z_h was computed. By means of a non-linear regression analysis the following $Z-R$ relation was obtained for C-band:

$$R_{Zh} = 7{\cdot}27 \times 10^{-2}\, Z_h^{0{\cdot}62} \tag{1}$$

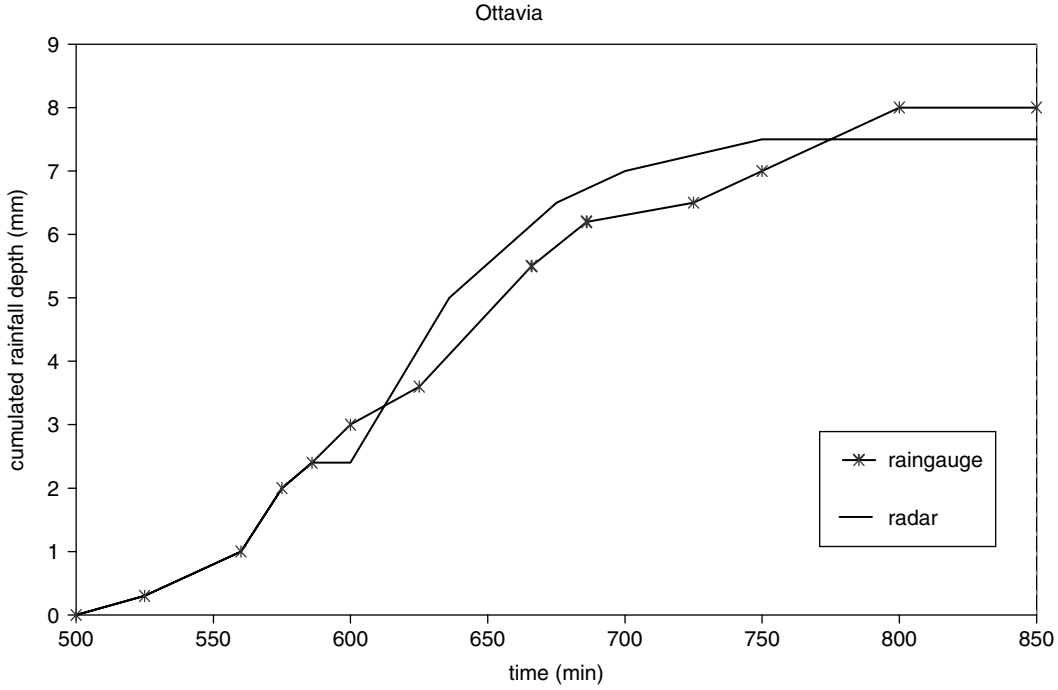

Figure 5. Time series of accumulated rainfall constructed for 'Ottavia' raingauge and the corresponding radar estimates at the gauge location

where Z is the reflectivity factor (dBZ) and R_{Zh} is rainfall (mm h^{-1}). The radar estimates are then averaged over the nearest neighbours up to 1 km on either side to obtain averaged measurements. This is done to smooth the data over measurement errors. The rainfall obtained from the radar over time is then integrated either in time or in space.

Rainfall fields comparison

In this subsection a comparative study of rainfall fields estimated using inverse-distance and kriging interpolation for the raingauge data and using radar measurements is presented. First of all a grid consisting of 900 cells was created over the city of Rome, with a mesh dimension of $2{\cdot}0 \times 2{\cdot}0$ km^2, in such a way that the three rainfall estimations were computed on these cells.

The first method used to estimate the rainfall field with measures of the 32 raingauges available consists in the interpolation of rainfall data using an inverse-distance technique (isohyets method). The result for the case study event is shown in Figure 6.

The second method used was kriging. This is an optimizing interpolation technique using one variable to determine the estimated values (Hohn, 1988); in particular, it is a stochastic interpolation technique that determines an unbiased minimum-variance estimator at the precipitation grid point. The earliest application of the kriging technique to rainfall interpolation, and comparison with other interpolations, can be found in Creutin and Obled (1982). A kriging rainfall estimation R_{GK} is performed by:

$$R_{GK} = \sum_{i=1}^{n} \lambda_i R_{Gi} \tag{2}$$

where R_{Gi} is rainfall measured by raingauge, and λ_i is the kriging weight. These weights λ_i are calculated by minimizing the variances of the estimated rainfall. If the estimate is unbiased (summation of λ_i equals 1),

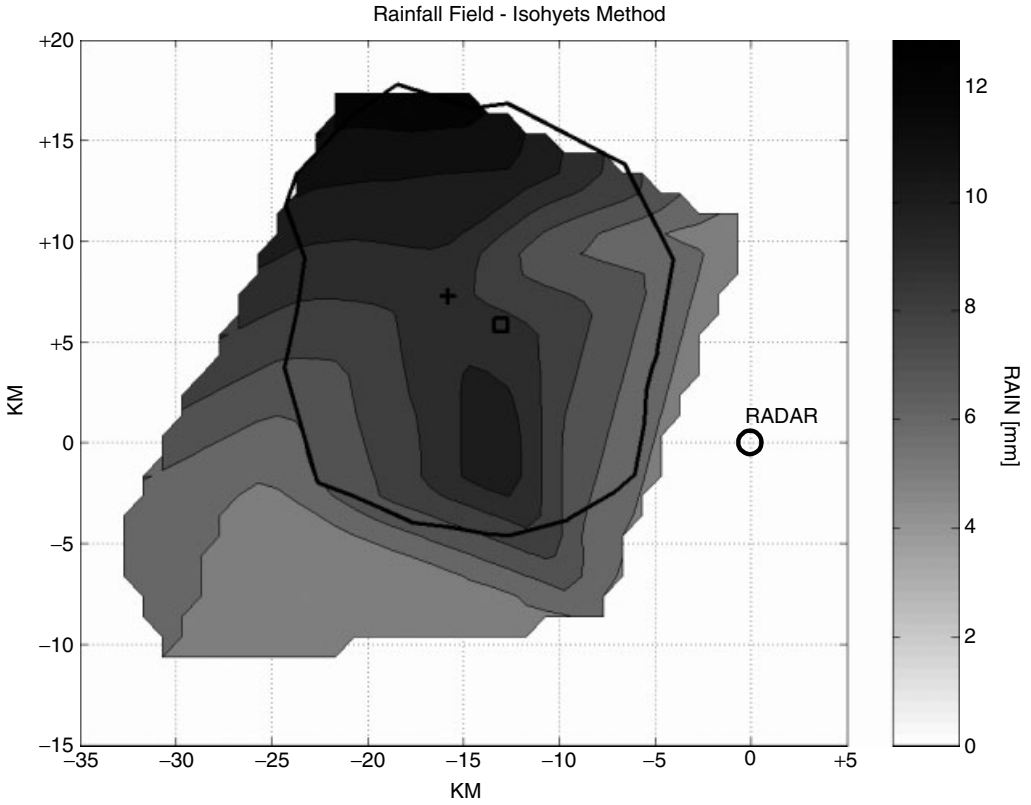

Figure 6. Rainfall field obtained with the interpolation of raingauge data using isohyets method. The distances (km) are referred to the radar site

Equation (2) leads to a minimization in the form:

$$\sum_{i=1}^{n} \lambda_i \gamma(v_i, v_j) + \mu = \gamma(v_i, V) \tag{3}$$

where the n weights λ_i are to be calculated and μ, a Lagrange parameter; v_i and v_j are locations between two known points; v_i and V are points between the known and estimated locations; γ is the semivariogram function.

To estimate the experimental semivariogram the distances between the gauges i and j are divided into $k = 6$ classes and then for each class k the value γ_K is computed as:

$$\gamma_K = \frac{\sum_{m=1}^{N_K} (R_{Gi} - R_{Gj})_m^2}{2N_K} \tag{4}$$

where N_K is the number of distances for the k-class. Computing the average distance d_K of the k-class, the experimental semivariogram is given by the coupled values $(d_K - \gamma_K)$ obtained for each class.

Finally, we fit the experimental points with a double exponential theoretical semivariogram, defined as:

$$\Gamma(d) = 1 - \left(c_0\, e^{-d/c_1} + (1 - c_0) e^{-d/c_2}\right) \tag{5}$$

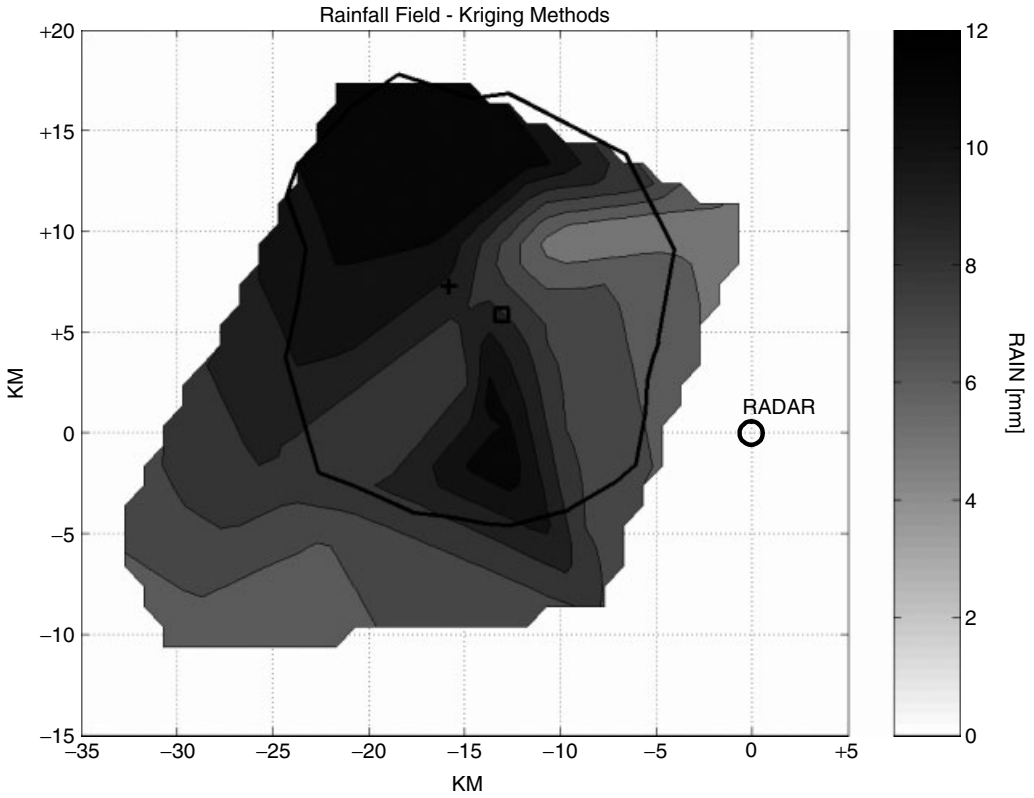

Figure 7. Rainfall field obtained with the interpolation of raingauge data using kriging. The distances (km) are referred to the radar site

where $c_0 = 0{\cdot}161$, $c_1 = 0{\cdot}337$ and $c_2 = 18{\cdot}827$ km. In this case, all 32 raingauges were used for the estimation of the rainfall field and the result is shown in Figure 7.

The third rainfall field was estimated by integrating in each cell of the grid all the radar measurements with the same technique used for the pointwise comparison. In Figure 8 the rainfall field estimated by radar is shown.

In order to evaluate the performance of the two interpolation methods, they were compared with the radar rainfall field using three objective functions: the mean absolute error (MAE), the root mean square error (RMSE) and the normalized standard error (NSE), defined as:

$$\mathrm{MAE} = \frac{1}{M}\sum_{i=1}^{M}|R_{Zhi} - R_{Gi}| \tag{6}$$

$$\mathrm{RMSE} = \sqrt{\frac{1}{M}\sum_{i=1}^{M}(R_{Zhi} - R_{Gi})^2} \tag{7}$$

$$\mathrm{NSE} = \frac{\sqrt{\dfrac{1}{M}\displaystyle\sum_{i=1}^{M}(R_{Zhi} - R_{Gi})^2}}{\dfrac{1}{M}\displaystyle\sum_{i=1}^{M}R_{Gi}} \tag{8}$$

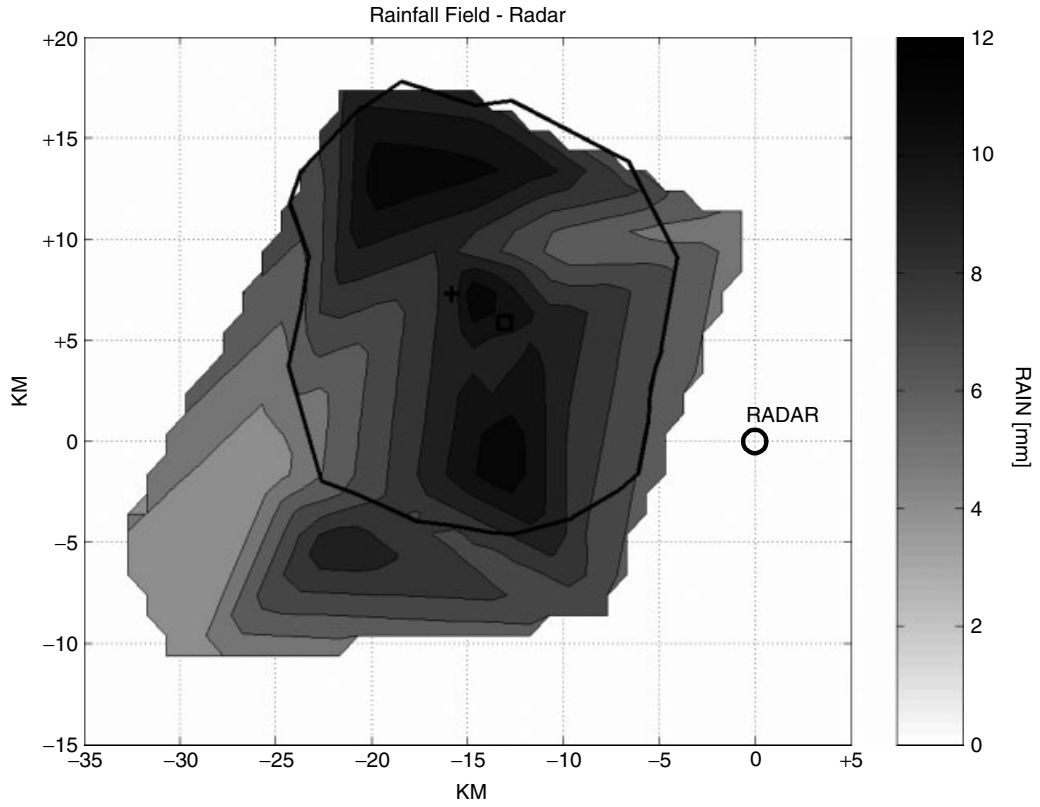

Figure 8. Rainfall field obtained by converting radar reflectivity factor to rainfall estimates. The distances (km) are referred to the radar site

where M is the number of cells, R_{Zhi} is the radar rainfall estimate and R_{Gi} the corresponding gauge data. In Table I the values of the three objective functions are summarized for the two interpolation methods: all the indicators give the lowest values for the kriging method.

Influence of raingauge network density

In order to quantify the influence of raingauge network density, three different scenarios are used with 8, 16 and 24 raingauges, respectively from the 32 available gauges. For each case it is possible to extract a number of different combinations C, given by:

$$C = \frac{n!}{k!(n-k)!} \tag{9}$$

where n is the total number of available raingauges and k is the number of gauges considered in the scenario. From a statistical point of view, for all three scenarios, characterized by a different number of elements,

Table I. Values of MAE, RMSE and NSE computed by comparison of rainfall fields obtained with isohyets method and kriging with the corresponding radar rainfall field

Objective functions:	MAE (mm)	RMSE (mm)	NSE
Isohyets–radar	1·62	1·94	0·32
Kriging–radar	1·51	1·85	0·31

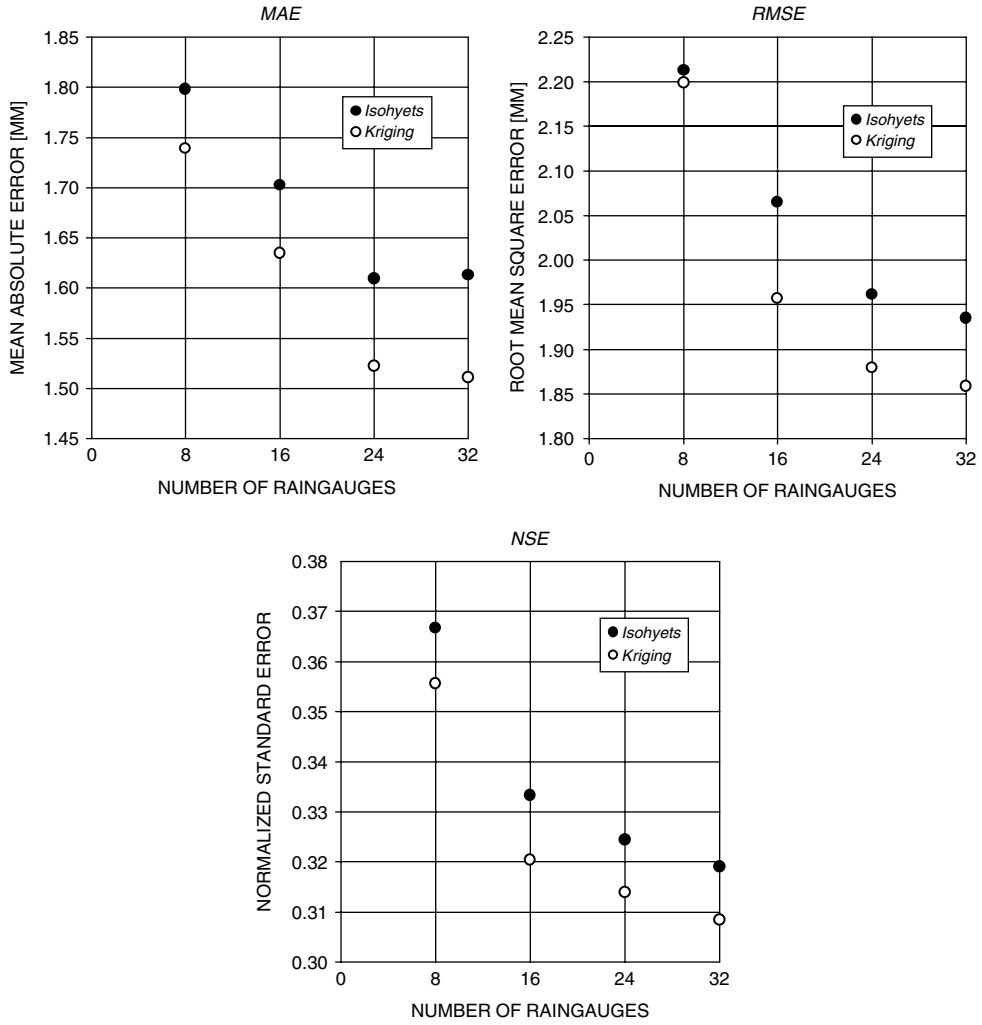

Figure 9. Trend of the mean absolute error (MAE), root mean square error (RMSE) and normalized standard error (NSE) with a different number of raingauges

only 50 combinations, randomly selected, are taken in order to quantify the performance as a function of the network density. For each scenario and for the entire network, the three objective functions (MAE, RMSE, NSE) were computed and are plotted in Figure 9.

For the three objective functions an asymptotic trend was pointed out: in particular, while a significant reduction of the differences between fields obtained with radar and raingauges is pointed out using 16 raingauges instead of 8, the difference using the entire network (32 raingauges) shows no relevant advantages with the use of 24 raingauges. However, in every case the use of geostatistical techniques leads to little improvement in comparison with isohyets methods.

SUMMARY AND CONCLUSION

A comparison between radar and raingauge measurements of rainfall over the city of Rome was presented in this paper. Radar operations for precipitation estimation are constrained by the requirements of avoiding beam

blockage as well as contamination by melting layer. A simple procedure was developed to remove errors in the area affected by ground clutter.

Data collected, after rejecting ground clutter, were analysed in two ways:

(a) Pointwise comparison of raingauge and radar estimates;
(b) Rainfall fields comparison with the application of isohyets and kriging interpolation for raingauge data.

To quantify the performance of the two interpolation methods, they were compared with the radar rainfall field using three objective functions (MAE, RMSE, NSE): for kriging all indicators give the best values.

Errors depending on the raingauge network density were weighed, changing the number of raingauges considered in the reconstruction of rainfall fields: three different scenarios were simulated, each one tested with 50 configurations. The increase in information with the raingauge density is computed, and it shows an asymptotic trend.

ACKNOWLEDGEMENTS

This research was supported partially by the National Group for Defence from Hydrogeological Hazards of the National Council of Research (GNDCI-CNR, Italy). The authors thank the National Hydrographic Service for providing the raingauge data.

REFERENCES

Anagnostou EN, Krajewski WF. 1999. Calibration of the WSR-88D precipitation processing subsystem. *Weather Forecasting* **13**: 396–406.
Aydin KT, Seliga TA, Balaji V. 1986. Remote sensing of hail with dual-linear polarization radar. *Journal of Climate and Applied Meteorology* **25**: 1475–1484.
Bastin G, Lorent B, Duque C, Gevers M. 1984. Optimal estimation of the average rainfall and optimal selection of raingauge location. *Water Resources Research* **28**(4): 1133–1144.
Borga M, Anagnostou N, Frank E. 2000. On the use of real-time radar rainfall estimates for flood prediction in mountainous basins. *Journal of Geophysical Research* **105**: 2269–2280.
Bras RF, Rodriguez-Iturbe I. 1976. Network design for the estimation of areal mean rainfall events. *Water Resources Research* **12**(6): 1185–1195.
Chua SH, Bras RF. 1982. Optimal estimation of mean areal precipitation in regions of orographic influences. *Journal of Hydrology* **57**: 713–728.
Creutin JD, Obled C. 1982. Objective analyses and mapping techniques for rainfall field: an objective comparison. *Water Resources Research* **18**: 413–431.
Dirks KN, Hay JE, Stow CD, Harris D. 1998. High-resolution studies of rainfall on Norfolk Island. Part II: Interpolation of rainfall data. *Journal of Hydrology* **208**: 187–193.
Finnerty BD, Smith MB, Seo DJ, Koren V, Moglen G. 1997. Space–time scale sensitivity of the Sacramento model to radar–gage precipitation inputs. *Journal of Hydrology* **203**: 21–38.
Fox NI, Collier CG, Tilford KA. 1999. Raingauge adjustment of radar measurements of stratiform rainfall. In *Proceedings of the XXIX International Conference on Radar Meteorology*, Montreal, Quebec, Canada.
Gorgucci E, Scarchilli G, Chandrasekar V. 1995. Radar and surface measurements of rainfall during CaPE. *Journal of Applied Meteorology* **34**: 1570–1577.
Gorgucci E, Scarchilli G, Chandrasekar V. 1996. Operational monitoring of rainfall over Arno river basin using dual-polarized radar and raingauges. *Journal of Applied Meteorology* **35**: 1221–1230.
Hohn ME. 1988. *Geostatistics and Petroleum Geology*. Van Nostrand Reinhold: New York; 264.
Krajewski WF. 1995. Rainfall estimation using weather radar and ground stations. In *Proceedings of the III International Symposium on Weather Radars*, San Paulo, Brazil.
Maheepala UK, Takyi AK, Perera BJC. 2001. Hydrological data monitoring for urban stormwater drainage systems. *Journal of Hydrology* **245**: 32–47.
Paoletti A. 1993. Effects of rainfall areal distribution on runoff volumes and peak flows. In *Proceedings U.S.–Italy Bilateral Seminar*, Water Resources Publications.
Pardo-Igùzquiza E. 1998. Optimal selection of number and location of rainfall gauges for areal rainfall estimation using geostatistics and simulated annealing. *Journal of Hydrology* **210**: 206–220.
Russo F, Gorgucci E, Napolitano F, Ubertini L. 2001. Radar rainfall estimates and raingauge measurements comparison: the Sesia basin case study during the Mesoscale Alpine Program. In *Proceedings of the III EGS Plinius Conference*, Baja Sardinia, Italy.

Steiner M, Smith JA, Burges SJ, Alonso CV, Darden RW. 1999. Effect of bias adjustment and rain gauge data quality control on radar rainfall estimation. *Water Resources Research* **35**(8): 2487–2503.

Todini E. 1995. The role of rainfall measurements and forecasts in real-time flood forecasting and management. In *Proceedings of the III International Symposium on Weather Radars*, San Paulo, Brazil.

Ulbrich CW. 1983. Natural variations in the analytical form of raindrop size distributions. *Journal of Climate and Applied Meteorology* **22**: 1764–1775.

Vaes G, Willems P, Berlamont J. 2001. Rainfall input requirements for hydrological calculations. *Urban Water* **3**: 107–112.

